Chapter 5

Adaptive Resonant Control

In this chapter, the natural frequency estimator from Chapter 4 is combined with the resonant controller from Chapter 3 to form a new adaptive resonant control (ARC) method. The ARC method is proposed to control systems with unknown loading conditions. The transient response of the ARC is then improved by combining it with the M^4RC method to form the proposed multi-model multi-mode adaptive resonant control (M^4ARC) method. This chapter begins with an introduction to adaptive control, with an emphasis given to transient response of adaptive control, and then it goes on to introduce a multiple model adaptive control method. The design of the proposed ARC and M^4ARC are presented in Section 5.2 and Section 5.3, respectively. The results from simulation studies and experimental studies are given in Sections 5.4 and 5.5, respectively.

5.1 Introduction

To achieve optimum attenuation in systems with varying parameters and unknown loading conditions, the adaptive resonant control method, ARC, is proposed. ARC is formed by combining the resonant controller discussed in Chapter 3 with the on-line natural frequency estimator presented in Chapter 4.

The on-line parameter estimator makes use of a recursive algorithm to identify

the plant parameters. The recursive algorithm uses previously estimated parameters as a starting point to predict the new parameters. Due to its recursive characteristic, the estimator can easily track variations to the plant parameter if they change gradually. In this situation, the adaptive control system will give optimum performance with an acceptable transient response. However, for large and sudden changes to the load in a mechanical system [64, 65] the recursive characteristic of the estimator will produce a large transient response. This transient response in the estimator will in turn generate an unacceptable transient response in the adaptive control system [30, 41, 50, 157].

To improve the transient response of adaptive control, the multiple model method with supervisor scheme presented in Chapter 3 can be combined with the adaptive control method to form the Multiple Model Adaptive Control (MMAC) method as proposed by Narendra and Balakrishnan [100]. This method assumes a set of L fixed-parameter models (M_1 to M_L) each representing an *a priori* known plant condition, and an adaptive model (M_a) to accommodate unmodeled plant conditions. The block diagram of this method is shown in Fig. 5.1. For each model $M_i(i = 1, 2, , L, a)$, a controller $K_i(i = 1, 2, , L, a)$ is designed to satisfy the control objective for M_i. At every sampling instant, each model, both fixed-parameter and adaptive, produces its own output $\widetilde{y}_i(i = 1, 2, , L, a)$ which is fed into a switching scheme (i.e., a supervisor). The supervisor selects between these controllers based on a MMSE performance index described in (3.34) or (3.35). Using this method, the supervisor will choose the most appropriate fixed-parameter model and its corresponding controller while the adaptive model is still in the transient phase, and then switch to and stay with the adaptive controller once its parameters have come out of their transient phase. The fixed-parameter models can provide speed whenever their parameters are close to those of the plant, while the adaptive model can provide accuracy because its parameters can be fine-tuned to match those of the plant.
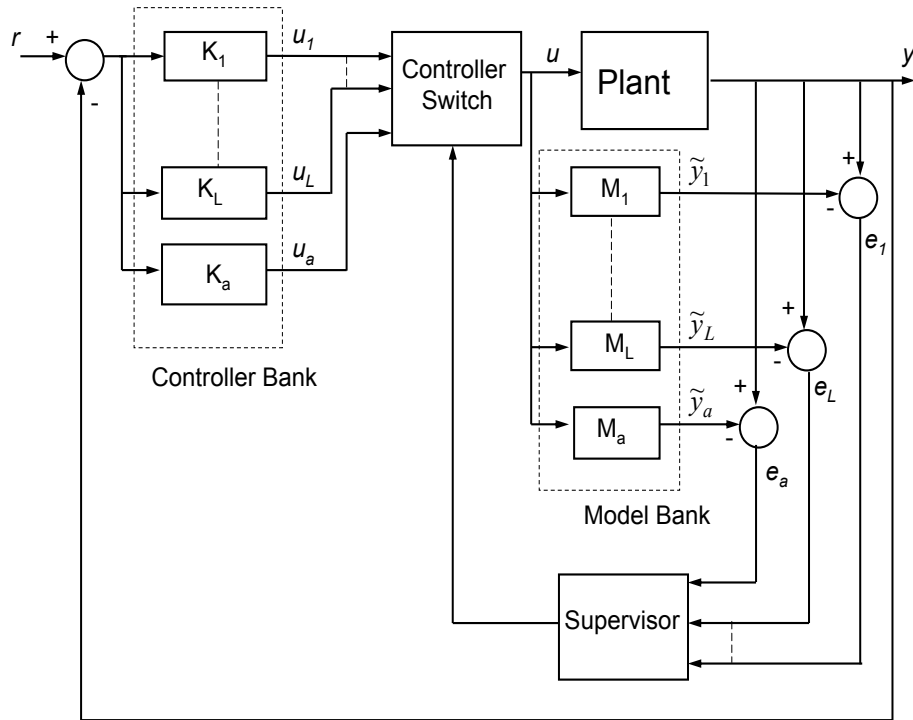
Figure 5.1. Block diagram of the MMAC.

The theory of MMAC is well developed. The stability proof of MMAC for a continuous system is given in [75, 101]. The method is extended to discrete-time linear systems in the presence of a disturbance in [105] and a proof of overall system convergence is offered. The method is also extended to stochastic systems [103, 159], non-linear systems [23, 62, 104] and non-minimum phase systems [149].

The MMAC concept has been applied to a broad range of applications that includes: flexible transmission systems [64], automobiles [62], robotics [102] and chemical processes [38, 39]. All of these applications use the MMSE performance index (3.34) or (3.35) for the supervisor scheme. As discussed in Chapter 3, this supervisor scheme imposes a high computational demand that increases significantly with the number of models. In this research, the MMAC concept is modified to improve the transient response of the proposed ARC.

The transient response of the ARC is improved by integrating it with the M^4RC method discussed in Chapter 3. The resultant M^4ARC uses a simple

supervisor scheme based on the utility of a filter bank system and the measurement of the output of the natural frequency estimator. The performance of the proposed controller is evaluated by comparing the M[4]RC, ARC, and M[4]ARC methods through simulation and experimental studies.

5.2   Adaptive Resonant Control (ARC)

The ARC is implemented using the indirect self tuning regulator (STR) scheme. The block diagram for controlling the first three modes of vibration is shown in Fig. 5.2. The figure shows that the ARC is formed by combining a natural frequency estimator with a resonant controller. The adjustable controller parameters for each mode are updated independently.
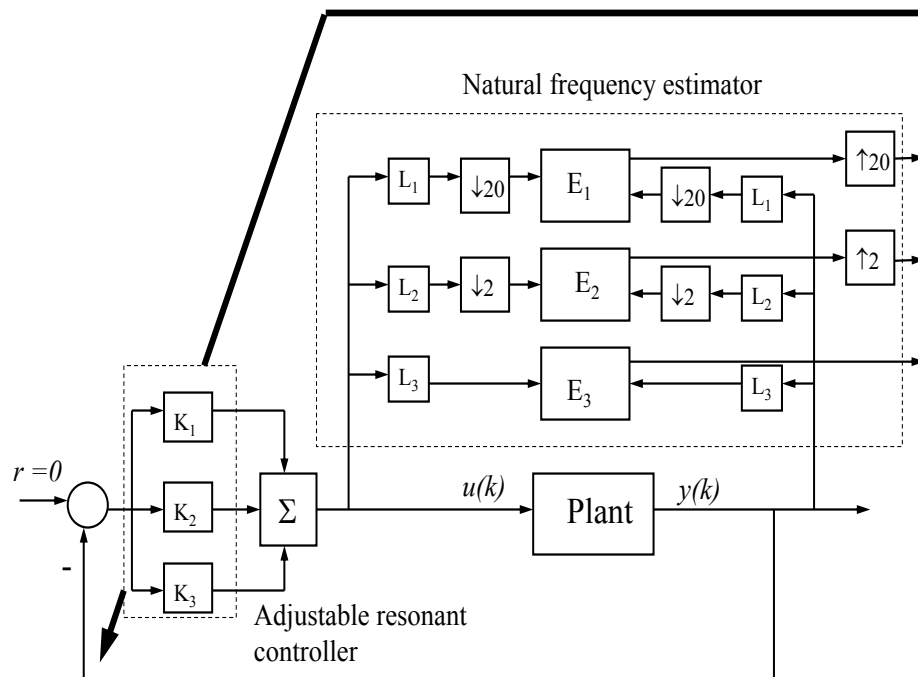

Figure 5.2. Block diagram of the ARC for controlling three modes.

ARC Algorithm

The algorithm for each mode is described by the following recursive process:

1. Sample the plant output $y(k)$.

2. Compute the control signal $u_m(k)$ using (3.13)

$$u_m(k) = A_m y(k) + B_m y(k-1) + C_m y(k-2) - D_m u_m(k-1) - E_m u_m(k-2).$$
(5.1)

3. Send the control signal $u_m(k)$ to the plant.

4. Compute $\hat{\omega}_m(k)$ using (4.68)

$$\hat{\omega}_m = 2f_s\sqrt{\frac{1 + a_{1m} + a_{2m}}{1 - a_{1m} + a_{2m}}}.$$
(5.2)

5. Update the controller parameters A_m, B_m, C_m, D_m and E_m using (3.7) - (3.11).

$$A_m = \frac{4f_s^2 + 4f_s\zeta_{cm}\omega_m}{4f_s^2 + 4f_s\zeta_{cm}\omega_m + \omega_m^2},$$
(5.3)

$$B_m = \frac{-8f_s^2}{4f_s^2 + 4f_s\zeta_{cm}\omega_m + \omega_m^2},$$
(5.4)

$$C_m = \frac{4f_s^2 - 4f_s\zeta_{cm}\omega_m}{4f_s^2 + 4f_s\zeta_{cm}\omega_m + \omega_m^2},$$
(5.5)

$$D_m = \frac{2\omega_m^2 - 8f_s^2}{4f_s^2 + 4f_s\zeta_{cm}\omega_m + \omega_m^2},$$
(5.6)

$$E_m = \frac{4f_s^2 - 4f_s\zeta_{cm}\omega_m + \omega_m^2}{4f_s^2 + 4f_s\zeta_{cm}\omega_m + \omega_m^2},$$
(5.7)

The final control signal $u(k)$ is the summation of the control signal for each mode as in (3.12)

$$u(k) = \sum_{m=1}^{M} u_m(k)k_{dm}.$$
(5.8)

Closed-loop stability of ARC

The ARC algorithm shows that the adaptation of the controller parameters for an indirect adaptive control method is achieved in two steps: (i) estimation of the plant parameters (step 4), and (ii) computation of the controller parameters based on the estimated plant parameters (step 5). The resulting control method should guarantee that the output of the plant remain bounded for bounded input if separately the three following conditions are satisfied: (i) the plant parameter estimates are bounded, (ii) the controller parameters are bounded for bounded plant parameter estimates, and (iii) the estimated plant parameters are admissible with respect to the control design strategy [70].

The first and second conditions are satisfied by using a stable estimator and controller, respectively. The third condition is necessary due to the fact that even the estimated plant parameters are bounded at each time t. The current estimated parameters may not be admissible in the sense that there is no solution for the controller. This is known as a singularity problem. For example, estimated parameters which cause a pole-zero cancellation cannot be used to compute the controller in the pole-placement control method.

The stability of the resonant controller and the natural frequency estimator was proven in Chapter 3 and Chapter 4, respectively. Thus only the admissibility of the parameters from the estimator needs to be proven to guarantee the stability of the ARC.

The stability proof of the resonant controller in Chapter 3 shows that the controller will produce a solution for any positive natural frequency, ω_m. Thus, the admissibility of the estimated parameters can be guaranteed by proving that the natural frequency estimator always produces a positive output.

Estimated parameters admissibility proof

Consider the estimated natural frequency (4.68) which is obtained from a

comparison of the transfer function of a flexible structure (2.32) with the bilinear transformation of a second-order discrete time system (4.65), as shown in Chapter 4. For convenience rewrite (4.68), (4.65), and (2.32) here

$$\omega_m = 2f_s\sqrt{\frac{1 + a_{1m} + a_{2m}}{1 - a_{1m} + a_{2m}}}, \tag{5.9}$$

$$G_m(z) = \frac{b_{1m}z + b_{2m}}{z^2 + a_{1m}z + a_{2m}}, \tag{5.10}$$

$$G(s, x) = \sum_{m=1}^{\infty} \frac{y_m(x)P_m}{s^2 + 2\zeta_m\omega_m s + \omega_m^2}. \tag{5.11}$$

The admissibility of the estimated parameters is guaranteed if the term within the square root operator of (5.9) is positive.

$$\frac{1 + a_{1m} + a_{2m}}{1 - a_{1m} + a_{2m}} > 0. \tag{5.12}$$

The inequality (5.12) is valid if both its numerator and denominator are positive or negative. To find a formulation of coefficients a_{1m} and a_{2m} in terms of the structure parameters ω_m and ζ_m, apply the bilinear transformation

$$s = 2f_s\frac{z - 1}{z + 1} \tag{5.13}$$

to (5.11) and compare the result with (5.10) to obtain

$$a_{1m} = \frac{2\omega_m^2 - 8f_s^2}{4f_s^2 + 4f_s\zeta_m\omega_m + \omega_m^2}, \tag{5.14}$$

$$a_{2m} = \frac{4f_s^2 - 4f_s\zeta_m\omega_m + \omega_m^2}{4f_s^2 + 4f_s\zeta_m\omega_m + \omega_m^2}. \tag{5.15}$$

From (5.14) and (5.15), the numerator and denominator of (5.12) can be written as

$$\begin{aligned}
num &= 1 + a_{1m} + a_{2m} \\
&= \frac{4f_s^2 + 4f_s\zeta_m\omega_m + \omega_m^2}{4f_s^2 + 4f_s\zeta_m\omega_m + \omega_m^2} + \frac{2\omega_m^2 - 8f_s^2}{4f_s^2 + 4f_s\zeta_m\omega_m + \omega_m^2} \\
&\quad + \frac{4f_s^2 - 4f_s\zeta_m\omega_m + \omega_m^2}{4f_s^2 + 4f_s\zeta_m\omega_m + \omega_m^2} \\
&= \frac{4\omega_m^2}{4f_s^2 + 4f_s\zeta_m\omega_m + \omega_m^2} > 0
\end{aligned} \tag{5.16}$$

and

$$
\begin{aligned}
den &= 1 - a_{1m} + a_{2m} \\
&= \frac{4f_s^2 + 4f_s\zeta_m\omega_m + \omega_m^2}{4f_s^2 + 4f_s\zeta_m\omega_m + \omega_m^2} - \frac{2\omega_m^2 - 8f_s^2}{4f_s^2 + 4f_s\zeta_m\omega_m + \omega_m^2} \\
&\quad + \frac{4f_s^2 - 4f_s\zeta_m\omega_m + \omega_m^2}{4f_s^2 + 4f_s\zeta_m\omega_m + \omega_m^2} \\
&= \frac{16f_s^2}{4f_s^2 + 4f_s\zeta_m\omega_m + \omega_m^2} > 0
\end{aligned}
\tag{5.17}
$$

respectively. From (5.16) and (5.17), it can be seen that both the numerator and denominator of (5.12) are always positive which implies that the admissibility of the parameter from the estimator is guaranteed. Therefore, by separately proving the stability of the estimator and the controller, and proving the admissibility of the parameter from the estimator, the ARC is proven to be stable.

5.3 Multi-model Multi-mode Adaptive Resonant Control (M^{4}ARC)

The M^{4}ARC method is proposed to facilitate the handling of fast transients in dynamic systems. M^{4}ARC combines the adaptive capability of the ARC with the fast response feature of M^{4}RC from Chapter 3. M^{4}ARC retains the characteristic of the M^{4}RC and ARC in that each mode is controlled independently. In the M^{4}ARC method, the system chooses a fixed-parameter model from the M^{4}RC method to deal with the transient condition while the adaptive model from the ARC method is still fluctuating. The system then switches to the adaptive model once the estimator has reached the vicinity of its steady state. To determine the condition of the mth mode estimator, the following convergence criterion is used.

$$
|\hat{\omega}_m(k) - \hat{\omega}_m(k-1)| \leq \delta_m
\tag{5.18}
$$

where k is the time base and δ_m is a positive small number. Using this convergence criterion, the supervisor scheme (3.35) can be simplified to (5.18) in the M^{4}ARC

method. The value of δ_m is obtained empirically. If δ_m is large then the supervisor will switch to the estimated parameters faster. However, if δ_m is too large the supervisor may select the estimator's outputs while they are still too far from the steady-state condition. This results in poor transient performance.

The block diagram of M^{4}ARC for controlling the first three modes of vibration is shown in Fig. 5.3. The figure shows that for each mode, a supervisor is used to update the parameters of the adjustable controller. The parameter from the natural frequency estimator, $\hat{\omega}$, is loaded into the adjustable resonant controller if criterion (5.18) is satisfied, otherwise the parameter from the closest fixed-parameter model to the current loading condition, $\overline{\omega}$, is loaded into the controller.
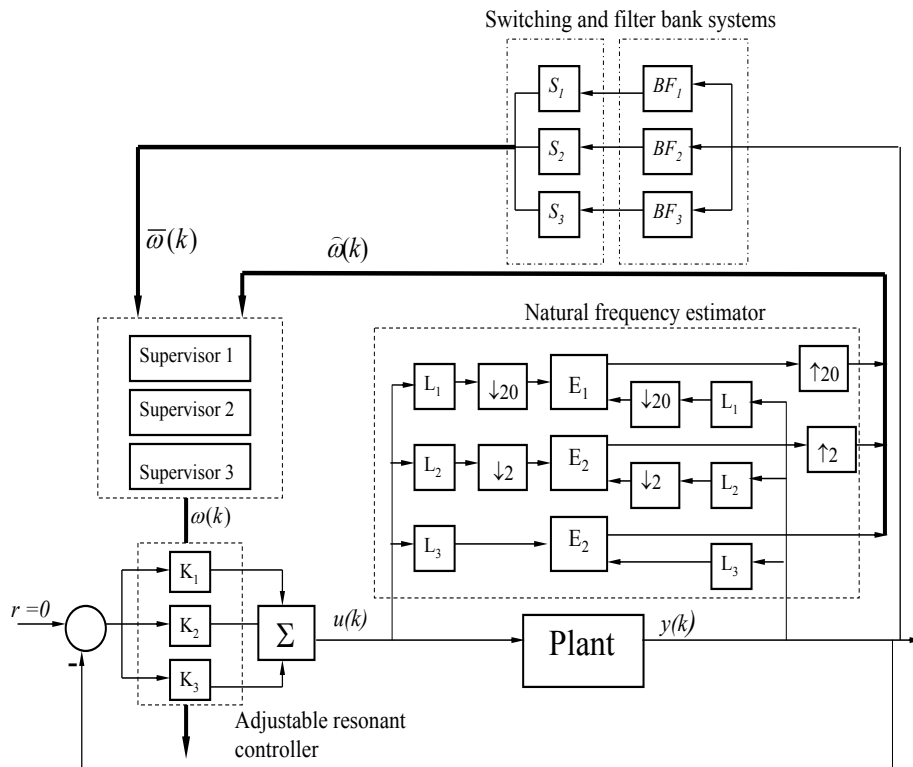

Figure 5.3: Block diagram of the M^{4}ARC for controlling three modes.

The filter bank system and switching system are the same as those in the M^{4}RC method shown in Fig. 3.10 and Fig. 3.11, respectively. In the M^{4}RC

method, as stated in Section 3.5.2, a large number of fixed-parameter models
is required to span an operating region if all the possible loads are not *a priori*
known. Because of the two following reasons, however, the number of fixed-
parameter models in the M^{4}ARC method can be significantly reduced.

1. The inclusion of an adaptive model. Because an adaptive model can change
   its parameters, it can span a very large operating region. Therefore, once
   the steady-state condition is achieved, one adaptive model can accurately
   represent all of the possible loading conditions in the operating region.

2. The use of wide band band-pass-filters in the filter bank to represent the
   fixed-parameter models. In the M^{4}ARC method, the fixed-parameter mod-
   els are used only to handle the transient conditions while the accuracy of
   the model to represent the loading conditions is handled by the adaptive
   model. Therefore, a band-pass-filter with a wider pass-band can be used in
   the filter bank. In this way a small number of fixed-parameter models can
   be used, as demonstrated in the following illustrative example.

Example 5.3.1

Similarly to Example 3.5.1, consider a resonant controller that is designed with
operating point 10 Hz and gain $k_d = 10$. Change the damping ratio from $\zeta_c =$
0.01 to $\zeta_c = 0.05$ to obtain a wider pass-band. The frequency response of the
controller is shown in Fig. 5.4. The figure shows that a gain of more than 32
dB is still achieved for a 1 Hz variation of the operating point. Assuming that
a controller with a gain of 32 dB gives acceptable attenuation, then one model
for every 2 Hz variation of the operating point is required, as shown in Fig. 5.5.
The band-widths of the operating region from the unload condition to the fully
loaded condition in the experimental plant for the first three modes are 4.5 Hz,
19.2 Hz, and 41.3 Hz, respectively. Therefore, to span the operating region of the

experimental plant the M^{4}ARC requires 3, 10, and 21 fixed-parameter models for the 1st, 2nd, and 3rd mode, respectively, or 34 models for the first three modes of vibration. Compared to the number of models required for the M^{4}RC method, as illustrated in example 3.5.1, the number of models required in the M^{4}ARC is significantly reduced from 650 to 34 (a 95% reduction).
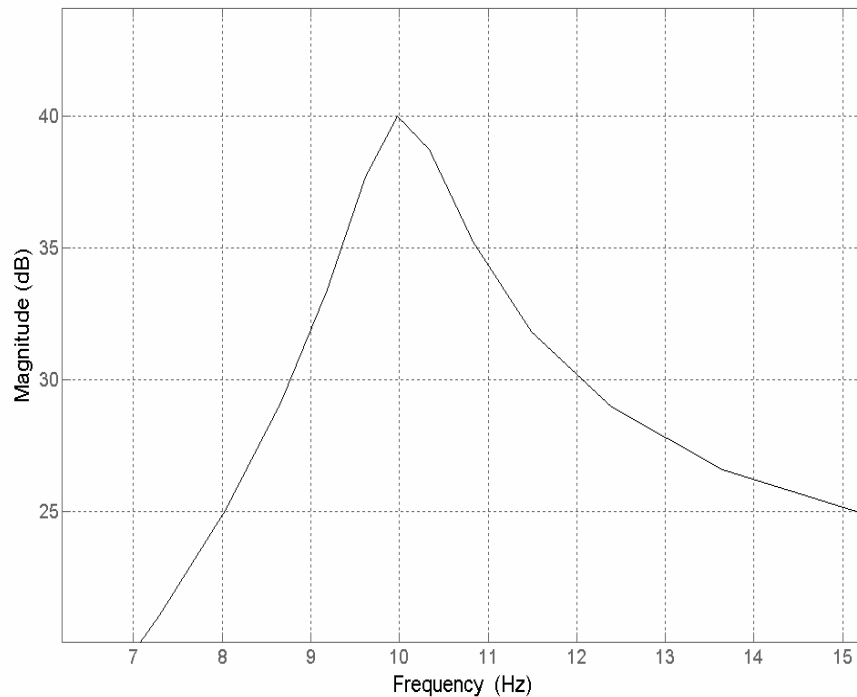

Figure 5.4: Frequency response of resonant controller with $\zeta_c = 0.05$ and $k_d = 10$.

M^{4}ARC algorithm

The M^{4}ARC algorithm for each mode is described by the following iterative procedure
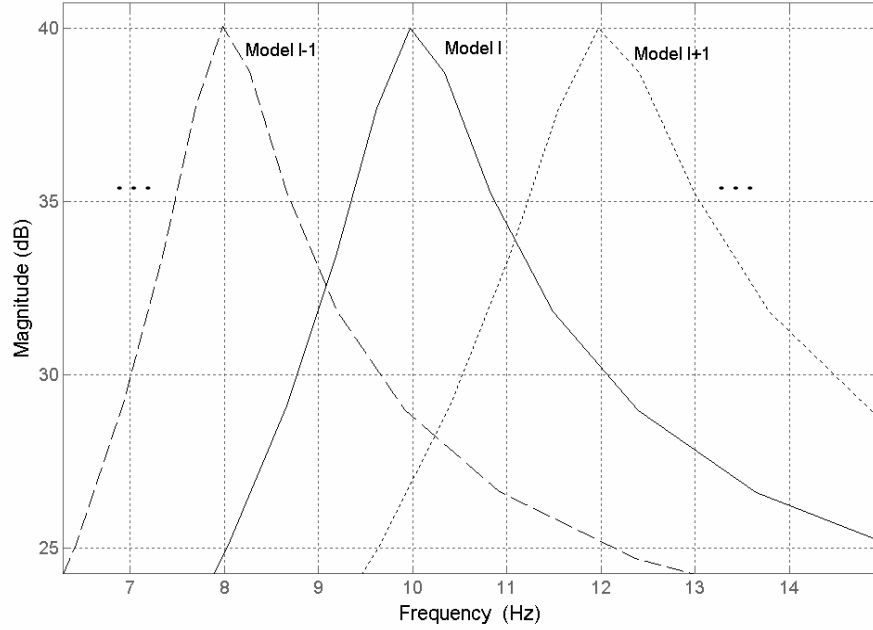
1. Sample the plant output $y(k)$.

Figure 5.5. Model array in the M^{4}ARC model bank.

2. Compute the control signal $u_m(k)$ using (3.13)

$$u_m(k) = A_m y(k) + B_m y(k-1) + C_m y(k-2) - D_m u_m(k-1) - E_m u_m(k-2).$$

(5.19)

3. Send the control signal $u_m(k)$ to the plant.

4. Compute $\hat{\omega}_m(k)$ using (4.68)

$$\hat{\omega}_m = 2f_s \sqrt{\frac{1 + a_{1m} + a_{2m}}{1 - a_{1m} + a_{2m}}}.$$

(5.20)

5. Compute $|\hat{\omega}_m(k) - \hat{\omega}_m(k-1)|$. If the result $\leq \delta_m$ then send $\hat{\omega}_m(k)$ to the controller else send $\overline{\omega}_m$ to the controller.

6. Update the controller parameters A_m, B_m, C_m, D_m and E_m using (3.7) - (3.11)

$$A_m = \frac{4f_s^2 + 4f_s \zeta_{cm}\omega_m}{4f_s^2 + 4f_s \zeta_{cm}\omega_m + \omega_m^2},$$

(5.21)

$$B_m = \frac{-8f_s^2}{4f_s^2 + 4f_s\zeta_{cm}\omega_m + \omega_m^2}, \tag{5.22}$$

$$C_m = \frac{4f_s^2 - 4f_s\zeta_{cm}\omega_m}{4f_s^2 + 4f_s\zeta_{cm}\omega_m + \omega_m^2}, \tag{5.23}$$

$$D_m = \frac{2\omega_m^2 - 8f_s^2}{4f_s^2 + 4f_s\zeta_{cm}\omega_m + \omega_m^2}, \tag{5.24}$$

$$E_m = \frac{4f_s^2 - 4f_s\zeta_{cm}\omega_m + \omega_m^2}{4f_s^2 + 4f_s\zeta_{cm}\omega_m + \omega_m^2}, \tag{5.25}$$

The final control signal $u(k)$ is the summation of control signal for each mode as in (3.12)

$$u(k) = \sum_{m=1}^{M} u_m(k)k_{dm}. \tag{5.26}$$

Closed-loop stability of M⁴ARC

Similar to M⁴RC method, the closed-loop stability of the M⁴ARC is guaranteed if it is assumed that the intervals between successive switches have a nonzero lower bound $T_{min} > 0$, which can be chosen to be arbitrarily small [100]. The condition in M⁴RC that there must be at least one controller in the controller bank that can stabilize the system is not necessary in M⁴ARC because this condition is automatically satisfied by the adaptive model once it comes close to the steady-state condition.

In the following sections, the effectiveness of the proposed ARC and M⁴ARC are evaluated through simulation and experimental studies.

5.4   Simulation Studies of ARC and M⁴ARC

In these simulation studies, the performances of the M⁴RC, ARC and M⁴ARC methods are evaluated using the dynamically loaded cantilevered beam. The simulation models of the plant, Model 1 to Model 4, are obtained from Chapter 2. The objectives of the simulation studies are twofold. Firstly, to demonstrate that in contrast to the M⁴RC, the ARC is able to optimally attenuate the plant

when the loading conditions are unknown. Secondly, to demonstrate that the M⁴ARC can improve the transient performance of the ARC when there are large and sudden changes to the plant parameters.

To achieve these two objectives, three simulation cases, namely M⁴ARC.1, M⁴ARC.2, and M⁴ARC.3, are conducted. The M⁴ARC.1 case is designed to achieve the first objective while the M⁴ARC.2 and M⁴ARC.3 cases are designed to achieve the second objective. For all the cases, the M⁴RC, ARC and M⁴ARC are designed and implemented to control the first three-modes. Each of the modes in the M⁴RC and M⁴ARC is represented by a filter bank, and each filter bank contains three band-pass filters representing the known loading models: Model 1, Model 3, and Model 4, respectively. The loading condition is changed in accordance with the model sequences as shown in Table 5.1. The parameters k_{d1}, k_{d2}, and k_{d3} and ζ_1, ζ_2, and ζ_3 for all the controllers are the same as the parameters of the resonant controller described in Chapter 3. The natural frequency estimator of the ARC has the same parameters as the natural frequency estimator described in Chapter 4. To make sure that the supervisor selects the adaptive model when the model is close to the steady-state condition (that is, within 90% of the steady-state value), the parameters δ_1, δ_2, and δ_3 in (5.18) for the M⁴ARC are chosen to be 0.05 using a trial and error procedure. The sampling period T is 1 kHz. The excitation signal is a summation of three sinusoids representing the first three natural frequencies of the current model. Each sinusoid has an amplitude of 1 volt.

Case	Loading condition is represented by Model	BPFs in the filter bank of M⁴RC and M⁴ARC is based on Model
M⁴ARC.1	1→2→4	1,3,4
M⁴ARC.2	1→3→4	1,3,4
M⁴ARC.3	1→4→1	1,3,4

Table 5.1: Plant and controller configuration for three different simulation study cases.

M^{4}ARC.1 case

In the M^{4}ARC.1 case, model 2 is deliberately not represented in the three filter banks, so as to allow the performances of the controllers with unmodeled dynamics to be assessed. The responses of the three control methods in the time domain are shown in Fig. 5.6. Plots (a), (b), and (c) represent the response of the M^{4}RC, ARC and M^{4}ARC, respectively. The plots show that ARC and M^{4}ARC produce a comparable response, while the M^{4}RC fails to give the optimum attenuation when the Model 2 loading condition occurs. M^{4}ARC cannot improve the transient response of the ARC because all of the fixed-parameter models (i.e., Model 1, Model 3 and Model 4) in the filter bank are significantly different from Model 2. When the loading condition changes to model 4, however, it can be seen that M^{4}ARC improves the transient response of the ARC. The overshoot percentage and settling time are reduced from 685 % and 2.5 seconds, respectively in the ARC to 187 % and 0.6 seconds, respectively in the M^{4}ARC.

Figure 5.7 shows how the M^{4}ARC switches between models in response to parameter changes. For the sake of clarity, the behaviour of each mode controller is shown separately. Labels, 1 to 4, on the Y-axes refer to the known fixed-parameter models, and label 5 refers to the adaptive model. From the figure, it can be seen that for each mode the system switches to the controller with the closest matching centre frequency while the adaptive model is still in the transient phase. The system switches to the adaptive controller once the adaptive model reaches the steady-state condition.

M^{4}ARC.2 and M^{4}ARC.3 cases

In the M^{4}ARC.2 and M^{4}ARC.3 cases, all the loading conditions are represented in the filter bank. To demonstrate that transient response improvement is more significant for large changes, the loading condition is changed directly from Model 1 to Model 4 in the M^{4}ARC.3 case. This loading change produces larger param-
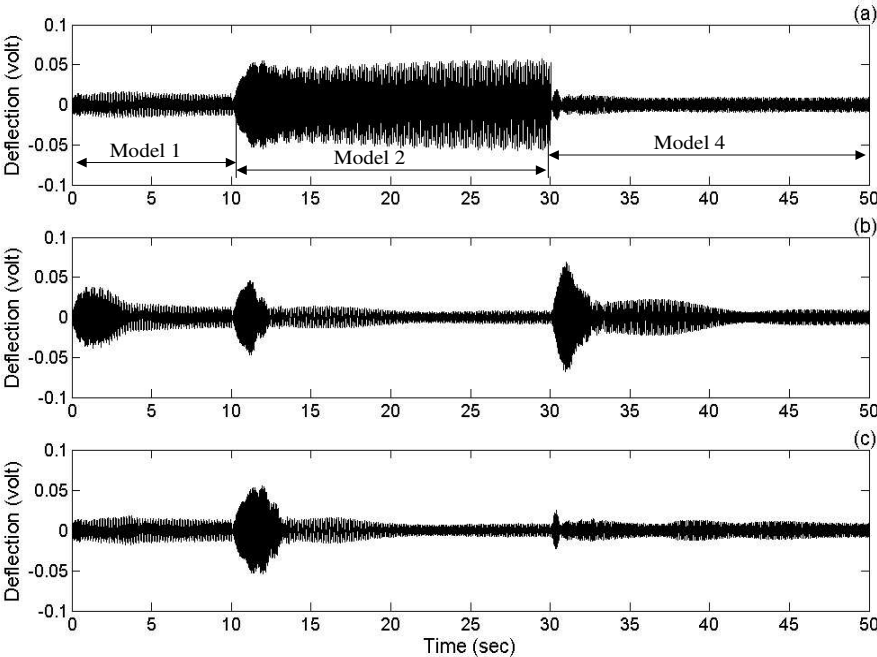
Figure 5.6: Simulation responses of the (a) M^4RC, (b) ARC and (c) M^4ARC for the $1 \rightarrow 2 \rightarrow 4$ model sequence.
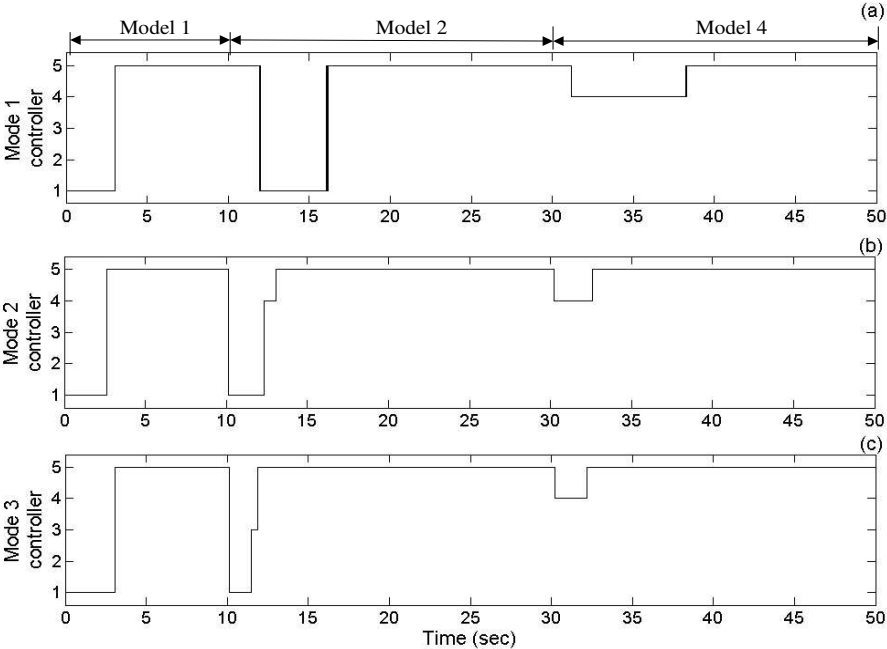

Figure 5.7: M^4ARC switching behaviour for the $1 \rightarrow 2 \rightarrow 4$ model sequence.

eter variations compared to when the loading condition changes gradually from Model 1 to Model 3 and then to Model 4, as in the M^{4}ARC.2 case.

Fig. 5.8 and Fig. 5.9 show the comparison of the three control methods for the M^{4}ARC.2 and M^{4}ARC.3 cases, respectively. From the figures, it can be seen that when all the loading conditions are included in the filter banks of the M^{4}RC and M^{4}ARC, both controllers give better transient performance than the ARC. The maximum overshoot percentage (M_o) and the settling time (T_s) of the ARC and M^{4}ARC for different loading model changes are shown in Table 5.2. The table shows that the M^{4}ARC improves the overshoot and settling time of the ARC when a large and sudden change occurs in the loading condition. The improvement is especially significant for the largest sudden change in the plant parameters when the loading condition changes from $1 \rightarrow 4$. This table also shows that the overshoot and settling time responses of the ARC when the loading conditions change from $1 \rightarrow 4$ and from $4 \rightarrow 1$ are significantly different. The overshoot response when the system releases the loads (i.e., change from Model 1 to Model 4) is larger than when the system picks up the loads (i.e., change from Model 4 to Model 1). This is because the damping of the system is decreased when the system releases the loads, causing a large overshoot. Conversely, the damping of the system is increased when the system picks up the loads and thus no large overshoot occurs even though the system experiences a large parameter variation.

	M_o (%)		T_s (seconds)	
Changes of Model	ARC	M^{4}ARC	ARC	M^{4}ARC
1→3	286	200	2.5	1
3→4	542	332	3	0.8
1→4	950	320	3.5	0.8
4→1	228	110	3.3	0.9

Table 5.2: Maximum overshoot percentage and settling time of ARC and M^{4}ARC for different loading changes.
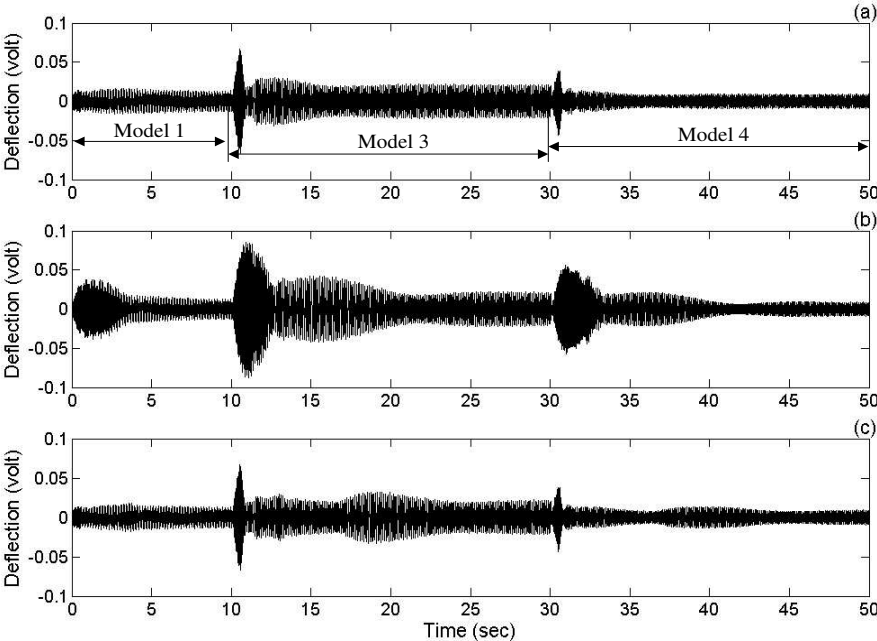
Figure 5.8: Simulation responses of the (a) M^{4}RC, (b) ARC and (c) M^{4}ARC for the $1 \rightarrow 3 \rightarrow 4$ model sequence.
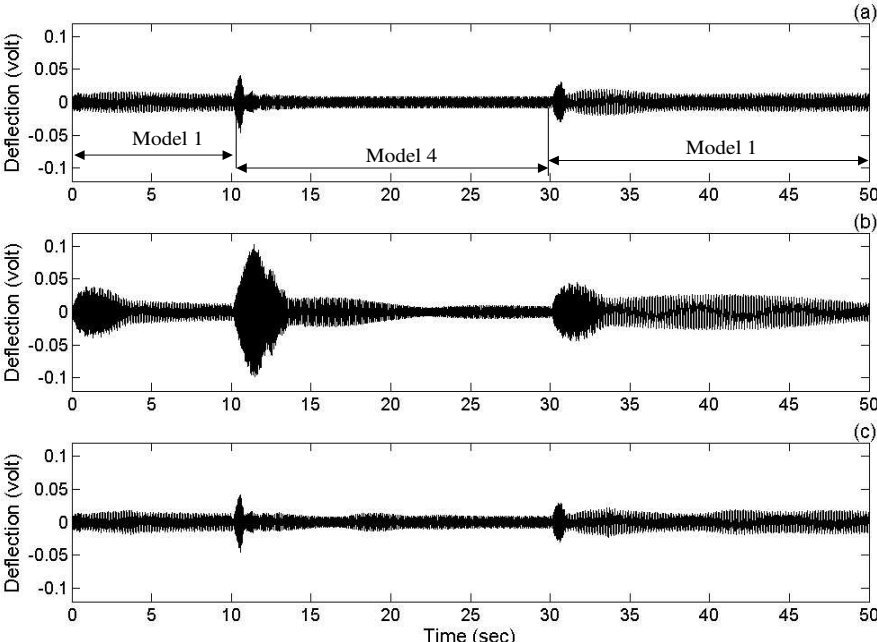

Figure 5.9: Simulation responses of the (a) M^{4}RC, (b) ARC and (c) M^{4}ARC for the $1 \rightarrow 4 \rightarrow 1$ model sequence.

The switching behaviour of the M[4]ARC for the M[4]ARC.2 and M[4]ARC.3 cases are shown in Fig. 5.10 and Fig. 5.11, respectively. Fig. 5.11 shows that when the loading is increased (i.e., $4 \rightarrow 1$), the controller continues to use the fixed-parameter model for a longer period than when the loading is decreased (i.e., $1 \rightarrow 4$). This behaviour shows that the estimator converges faster when the system releases the load as opposed to when the system picks up the load. The switching behaviour also reveals that as a result of the multi-rate sampling scheme, the estimators for the lower modes, which use a longer sampling period, take a longer time to settle than the estimators for the higher modes. Consequently with the M[4]ARC, the transient times for the lower modes are longer than those for the higher modes.
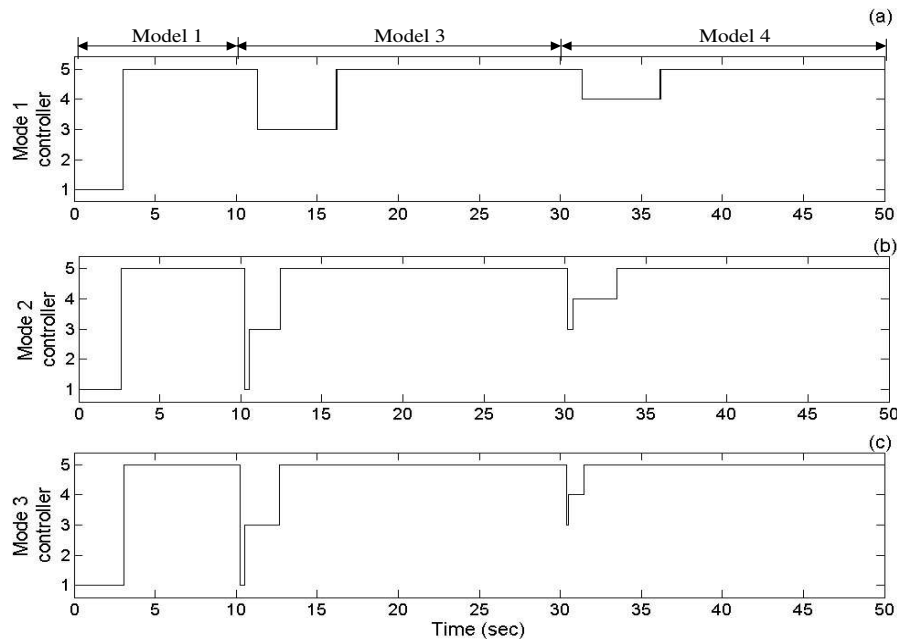

Figure 5.10: M[4]ARC switching behaviour for the $1 \rightarrow 3 \rightarrow 4$ model sequence.

From the simulation cases, it is observed that the M[4]RC gives the best performance if all the possible loading conditions are represented in the filter banks, but gives poor performance for unmodeled loading conditions. As expected, the
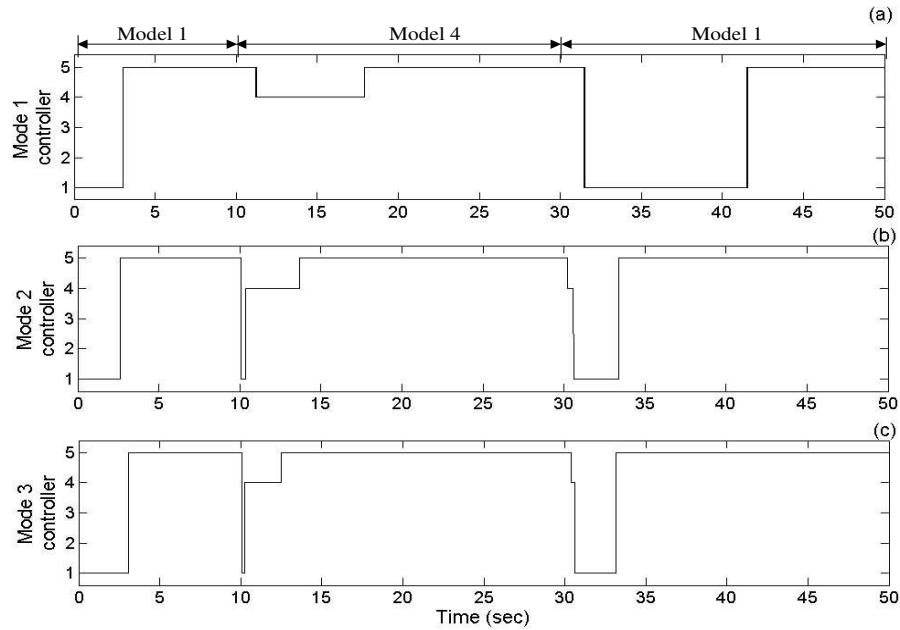
Figure 5.11: M^{4}ARC switching behaviour for the $1 \rightarrow 4 \rightarrow 1$ model sequence.

M^{4}ARC improves the transient response of the ARC when large and sudden changes in the loading conditions occur provided that at least one model in the filter bank is close enough to the new unknown loading condition. Since it is impractical in real applications to construct a fixed-parameter multi-model resonant controller that can accommodate all possible loading conditions and allow for drift of the model parameters, the M^{4}ARC method offers the best compromise in terms of transient performance and load matching.

5.5   Experimental Studies

To verify the results obtained from the simulations, the performances of the ARC, M^{4}RC, and M^{4}ARC are evaluated on the physical beam system in the following experiments. All the controllers used in the simulation studies are implemented on a dSPACE DS1103 data acquisition board using Matlab, Simulink, and Real-Time

Workshop software to build a real-time experiment. The schematic diagram of the experimental set-up is the same as that shown in Fig. 3.34 in Chapter 3. The three simulation cases $M^4ARC.1$ to $M^4ARC.3$ are repeated in the experiments. For the $M^4ARC.1$ and $M^4ARC.2$ cases in the experiments, however, the controllers are turned on and off at several instants to compare the open-loop and closed-loop responses of the three control methods. Furthermore, due to the limitation of the experimental apparatus, the $M^4ARC.3$ case in the experiments can only change the loading condition by releasing the load (i.e., Model $1 \rightarrow 4$), and not by picking up the load (i.e., Model $1 \rightarrow 4$).

$M^4ARC.1$ case

The performances of the three control methods are shown in Fig. 5.12. The figure shows that the performance of the M^4RC is very poor compared to those of the ARC and M^4ARC when the Model 2 loading condition is encountered. This case shows that the fixed-parameter controller M^4RC is unable to control unknown models. However when the loading changes to Model 4, it can be seen that the M^4RC and M^4ARC produce better transient performance than the ARC. The maximum overshoot and settling time of the systems are reduced from 607 % and 7 seconds, respectively, for the ARC to 362 % and 4 seconds, respectively, for the M^4ARC.

The switching behaviour of the M^4ARC is shown in Fig. 5.13. By the onset of each of the three load sequences, the natural frequency estimator has already determined the three mode frequencies before the controller is turned on - hence the adaptive model parameter set, 5, is initially selected for the adjustable controller. Fig. 5.13 reveals that for each mode the system selects the fixed-parameter model closest to the current loading conditions when the adaptive model is in the transient condition and switches to the adaptive model once the adaptive model reaches steady-state.
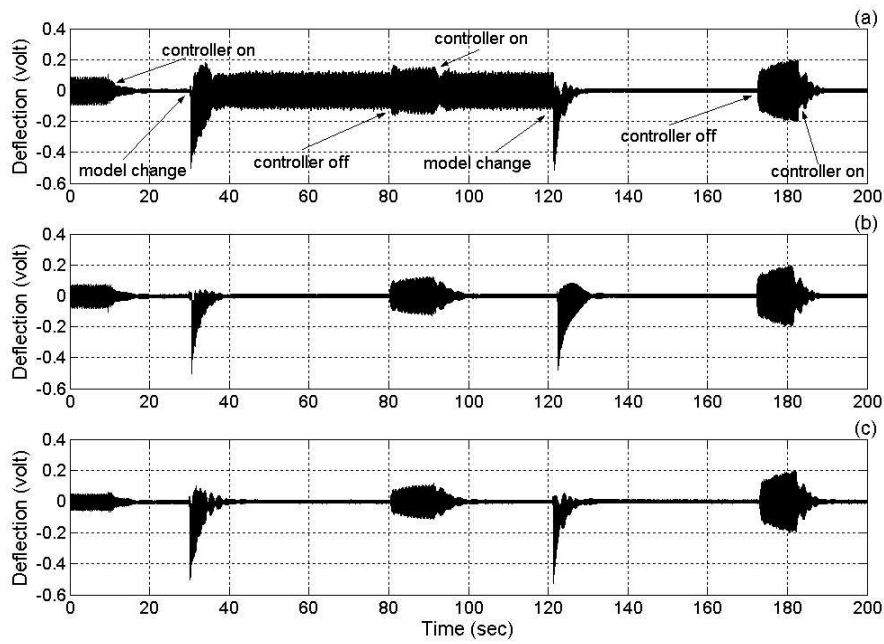
Figure 5.12: Responses of the (a) M^4RC, (b) ARC and (c) M^4ARC for the $1 \rightarrow 2 \rightarrow 4$ model sequence.
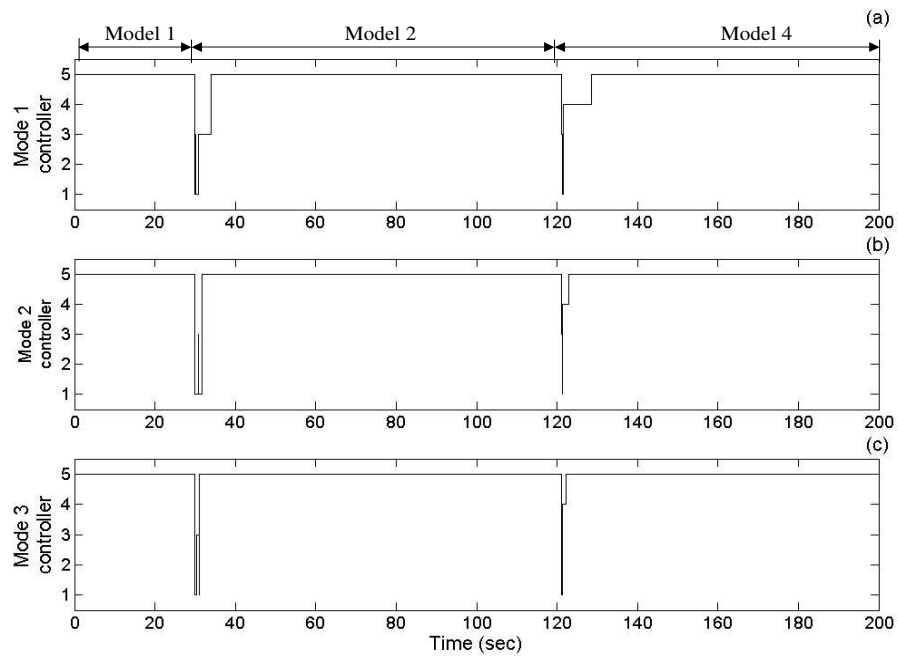

Figure 5.13: M^4ARC switching behaviour for the $1 \rightarrow 2 \rightarrow 4$ model sequence.

M^{4}ARC.2 and M^{4}ARC.3 cases

The performances of all the control methods for the M^{4}ARC.2 and M^{4}ARC.3 cases are shown in Figs. 5.14 and 5.15, respectively. Since all the loading conditions are represented in the filter banks of M^{4}RC and M^{4}ARC, both controllers give equally better performance than the ARC. The transient responses of the system, as measured by the overshoot and settling time, are improved with the M^{4}ARC relative to ARC, as is shown in Table 5.3. In the M^{4}ARC.2, when the loading condition changes from $1 \rightarrow 3$, the differences in performance between the three control methods are not as clear as when the loading condition changes from $3 \rightarrow 4$. This is because the changes in parameters from $1 \rightarrow 3$ are smaller than those from $3 \rightarrow 4$. However, when the loading changes to Model 4, M^{4}ARC outperforms ARC in terms of transient performances. This observation is reinforced in the M^{4}ARC.3 cases which produce the largest sudden changes in the plant parameters. The corresponding responses shown in Fig. 5.15 demonstrate that the M^{4}ARC has an improved transient performance relative to that of ARC.

	M_o (%)		T_s (seconds)	
Changes of Model	ARC	M^{4}ARC	ARC	M^{4}ARC
$1{\rightarrow}3$	359	253	3	3
$3{\rightarrow}4$	590	302	6	3
$1{\rightarrow}4$	478	239	8	7

Table 5.3: Maximum overshoot percentage and settling time of ARC and M^{4}ARC for different loading changes.

Figs. 5.16 and 5.17 show the controller switching behaviour for the three modes of the M^{4}ARC method for the M^{4}ARC.2 and M^{4}ARC.3 cases, respectively. Fig. 5.16 reveals that for the loading sequence $1 \rightarrow 3 \rightarrow 4$, the system momentarily switches to the fixed-parameter Model 1 when the load changes from $1 \rightarrow 3$, then switches to the fixed-parameter Model 3, before finally settling with the adaptive model, 5, once the adaptive model reaches steady-state. For the load
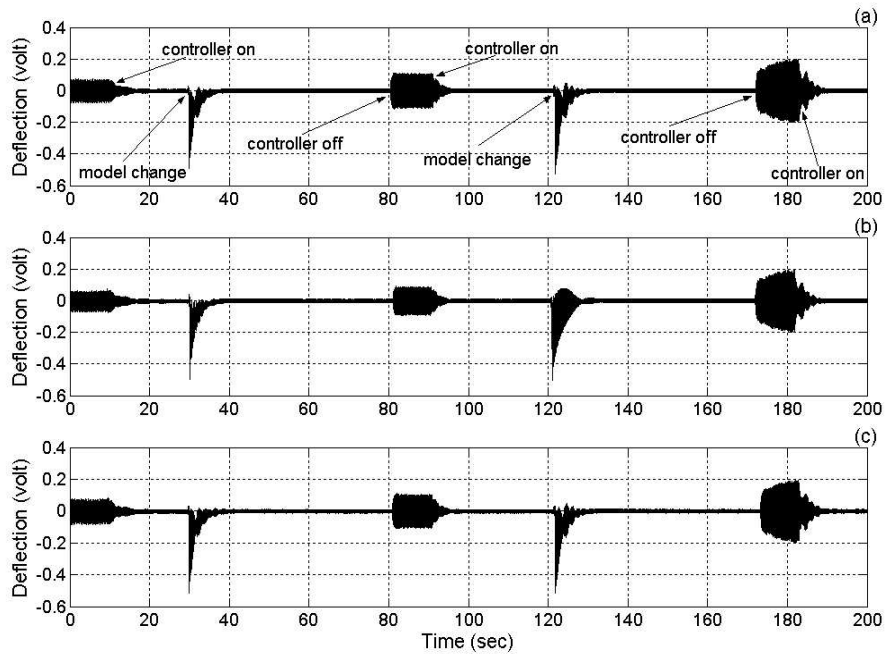
Figure 5.14: Responses of the (a) M^{4}RC, (b) ARC and (c) M^{4}ARC for the $1 \rightarrow 3 \rightarrow 4$ model sequence.
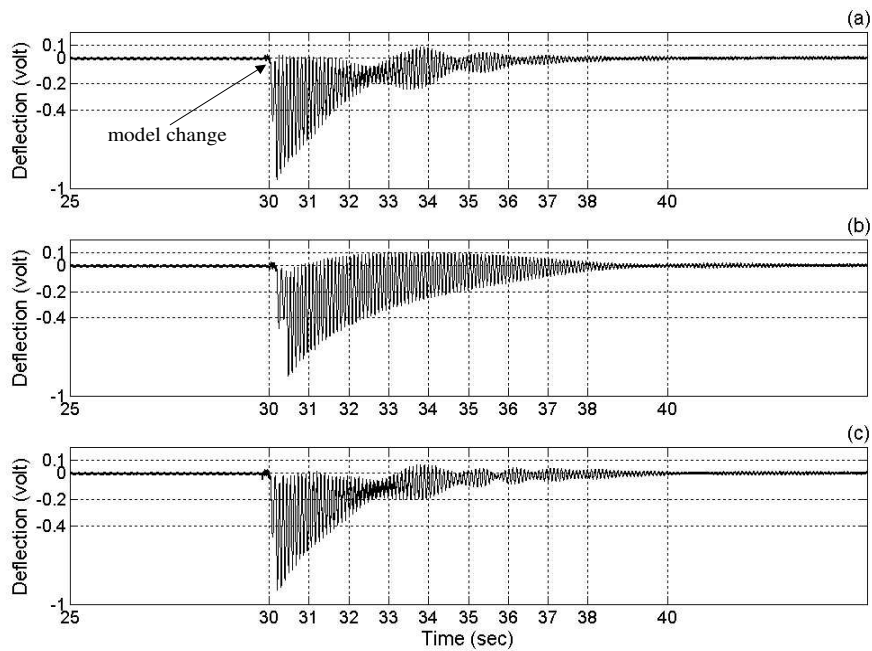

Figure 5.15: Responses of the (a) M^{4}RC, (b) ARC and (c) M^{4}ARC for the $1 \rightarrow 4$ model sequence.
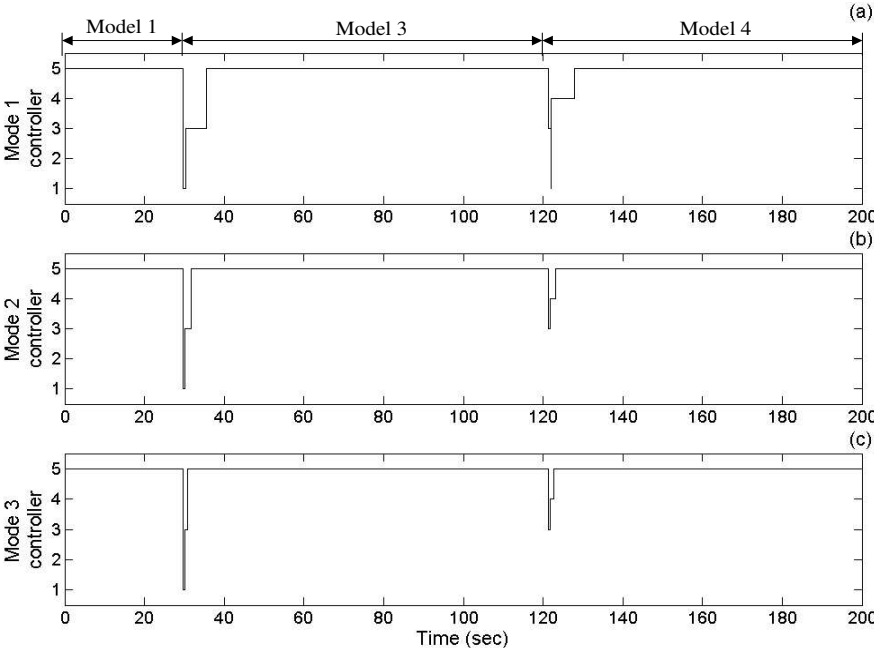
Figure 5.16: M^{4}ARC switching behaviour for the $1 \rightarrow 3 \rightarrow 4$ model sequence.
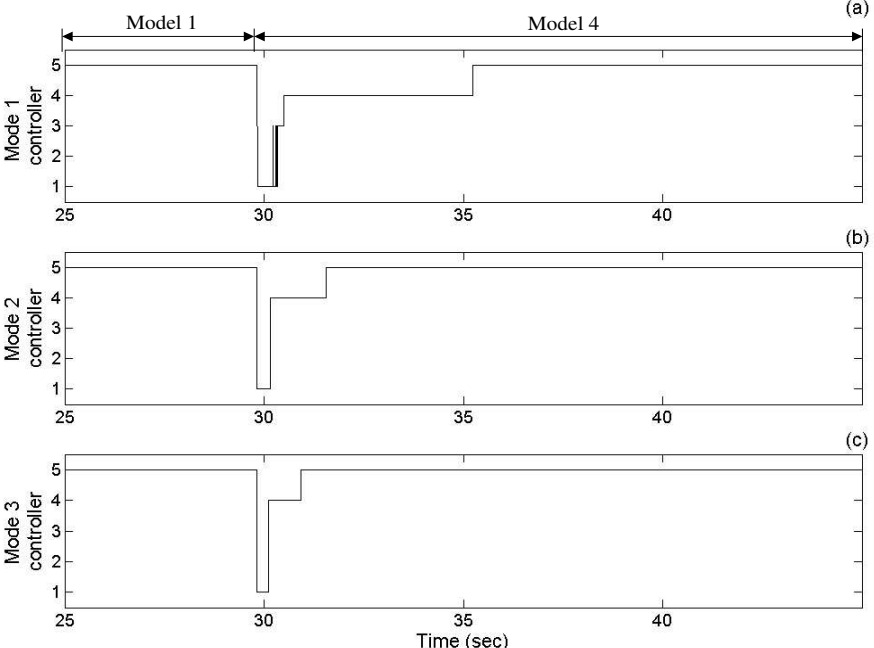

Figure 5.17: M^{4}ARC switching behaviour for the $1 \rightarrow 4$ model sequence.

change $3 \rightarrow 4$, the controllers for modes 2 and 3 first switch to the fixed-parameter Model 3, then to the fixed-parameter Model 4 before settling on the newly estimated adaptive model. Fig. 5.17 demonstrates the switching behaviour under the extreme loading change $1 \rightarrow 4$. For the first mode, the system switches from Model 1 to Model 3 and onto Model 4, whereas for modes 2 and 3, the controllers switch directly from Model 1 to Model 4. All the switching behaviours demonstrate that while the estimator is in the transient phase, each mode controller will independently switch to the model with centre frequencies that are closest to the frequencies of the vibration and then eventually switch to the estimated model parameters once the mode estimator attains steady-state. In agreement with the simulation results, the switching diagrams in the experimental results show that the estimator for the lower modes takes longer to settle than the estimator for the higher modes. The experimental results also reveal that the proposed switching scheme avoids undesirable rapid switching.

The experimental apparatus only allows the load(s) to be released. However, in principle the proposed methods should also work for systems with incremental loading, as shown in the M^{4}ARC.3 cases in the simulations.

5.6   Summary

In this chapter, the ARC method is proposed to improve the attenuation performance of resonant control by enabling it to control multi-mode vibration in systems with unknown loading conditions. The ARC method is necessary because the M^{4}RC method fails to give optimum performance for unknown loading conditions. The ARC method is developed by combining a resonant controller with a natural frequency estimator, and is implemented as an STR indirect adaptive control method. The M^{4}ARC method is then proposed to improve the ARC's transient response. The M^{4}ARC method is designed by including an adaptive

model in the M^{4}RC model bank. A simple supervisor, which makes use of a filter bank to identify the closest matching model and the measurement natural frequency estimator's output, is proposed to control the switching between the fixed-parameter models and the adaptive model. The proposed supervisor significantly reduces the computational load and avoids unwanted switching.

Simulations and experiments based on the dynamically loaded cantilever beam with multiple-frequency excitation demonstrate that the proposed ARC has good attenuation performance, while the proposed M^{4}ARC has both good attenuation performance and transient performance.

The proposed M^{4}ARC method provides a basis for a controller that with a minimum number of sensor-actuator pairs is robust to unmodeled dynamics, able to respond quickly to large and sudden load changes and is simple enough for real-time implementation. This method offers a solution to a broad range of control problems where a high performance controller working to stringent transient performance requirements is required to accommodate large variations to a system parameters.